遙感探測的應用

作者：鄭錦金
系級：都市計畫與空間資訊學系碩一
學號：M9945667

開課老師：楊龍士　嚴泰來 教授

課程名稱：遙感探測學專論

開課系所：土地管理

開課學年：　99　　學年度 第 1 學期

中文摘要

遙感探測對於環境監測與資源探勘提供了重要的貢獻。遙感探測的監測資料有四維的要素，其中是三維的空間資料及另一維則是時間的資料，不同的時間在同一地點所觀測到的資訊是有差異的。本報告的目的在於瞭解遙感探測的發展及其在各方面的應用。透過文獻回顧法，整理由 1992 年到 2010 年度中，抽取 10 篇國內外的期刊及論文，發現遙感探測的應用範圍非常之廣泛，其中包括觀測及分析冰原地表積雪融化及雪的累積狀況、透過 NDVI 值觀測糧食產量的變化情形、利用高光譜遙感反射率導數光譜去判別浮游植物色素的聚集分析、用氣象雷達之觀測資料與回饋式類神經網路建立定量降雨及洪水預報模式、觀測水稻含氮狀態進行分析、利用中解析度成像光譜儀(MODIS)去觀測雲、氣溶膠和水蒸氣的性質進行進一步分析。由於每一篇都屬於不同的研究，每一研究都有其結果的應用範圍和情況，在以下章節中一一說明。

關鍵字：Moderate Resolution Imaging Spectrometer (MODIS) ，NDVI，遙感探測 (Remote Sensing, RS)

目 次

Chapter1. 緒論

從搜尋資料開始，想找找遙感探測有史以來做過什麼應用，有過什麼貢獻，才赫然發現原來遙感探測起源于第一次世界大戰，老師說過所有最高科技，最精密的技術都是最先用在軍事及宗教上，果然是如此。遙感探測的技術演變到如今，已經不只是我們課堂所學的那麼基礎的理論那麼簡單了，透過文獻的搜尋，才知道遙感探測在我還沒出生或還在讀小學的時代就已經被應用的非常深澳及廣泛，只是我們都不知道罷了。但是我們課堂所學的那麼基礎的理論又是那麼重要，這樣才能幫助我們瞭解所參考的文獻的內容及理論。

以下表格是依年度排序的資料，是我所參考有關於遙感探測的應用的期刊或論，在以下每一章節中只貼上其摘要，針對該篇文獻寫了一些所看到的內容及心得。

表 1 遙感探測相關文獻整理表

年度	作者	研究題目
2010	Indrajit Bhattacharya	Analysis of Surface Melting and Snow Accumulation over the Greenland Ice Sheet from Spaceborne Microwave Sensors
2010	Cristina Milesi, Arindam Samanta , Hirofumi Hashimoto , K. Krishna Kumar , Sangram Ganguly , Prasad S. Thenkabail , Ashok N. Srivastava , Ramakrishna R. Nemani and Ranga B. Myneni	Decadal Variations in NDVI and Food Production in India
2009	E. Torrecilla, J. Piera1, D. Stramski, R. Reynolds, E. Millán-Nuñez	Identification of Phytoplankton Pigment Assemblages Using Derivative Spectroscopy of Hyperspectral Remote -Sensing Reflectances
2007	江衍銘、張斐章	以類神經網路建構定量降雨及多階段洪水預報模式
2007	李裕娟	圖繪田間水稻含氮狀態之遙感探測技術研究

年度	作者	研究題目
2006	Dong Huang, Yuri Knyazikhin , Robert E. Dickinson , Miina Rautiainen , Pauline Stenberg ,Mathias Disney , Philip Lewis , Alessandro Cescatti, Yuhong Tian , Wout Verhoef ,John V. Martonchik , Ranga B. Myneni	Canopy spectral invariants for remote sensing and model applications
2006	Faith Ann Heinsch, Maosheng Zhao, Steven W. Running, John S. Kimball, Ramakrishna R. Nemani, Kenneth J. Davis, Paul V. Bolstad, Bruce . Cook, Ankur R. Desai, Daniel M. Ricciuto, Beverly E. Law, Walter . Oechel, Hyojung Kwon, Hongyan Luo, Steven . Wofsy, Allison L. Dunn, J. William Munger, Dennis . Baldocchi, Liukang Xu, David Y. Hollinger, Andrew D. Richardson, Paul . Stoy, Mario . S. Siqueira, Russell K. Monson, Sean P. Burns, and Lawrence . Flanagan	Evaluation of Remote Sensing Based Terrestrial Productivity From MODIS Using Regional Tower Eddy Flux Network Observations
2000	計畫主持人：陳文福 執行單位：國立中興大學水土保持學系	行政院國家科學委員會專題研究計畫成果報告：結合遙測技術與地理資訊系統以建立集水區降雨資料之推估模式之研究(Ⅲ)
1998	Christopher O. Justice, Eric Vermote, , John R. G. Townshend, Ruth Defries, David P. Roy, Dorothy K. Hall, Vincent V. Salomonson, Jeffrey L. Privette, George Riggs, Alan Strahler, Wolfgang Lucht, Ranga B. Myneni, Yuri Knyazikhin, Steve W. Running, Rama R. Nemani, Zhengming Wan, Alfredo R. Huete, Wim van Leeuwen, Robert E. Wolfe, Louis Giglio, Jan-Peter Muller, Philip Lewis, and Michael J. Barnsley	The Moderate Resolution Imaging Spectroradiometer (MODIS): Land Remote Sensing for Global Change Research
1992	Michael D. King, Yoram J. Kaufman, W. Paul Menzel, and Didier Tanrk	Remote Sensing of Cloud, Aerosol, and Water Vapor Properties from the Moderate Resolution Imaging Spectrometer (MODIS)

Chapter2.Analysis of Surface Melting and Snow Accumulation over the Greenland Ice Sheet from Spaceborne Microwave Sensors

Abstract

Continuous monitoring of changes in the Greenland ice sheet from both space and air borne sensors has been conducted since the early 1970's. Since the mid-1990's dramatic changes occurring on the Greenland ice sheet have been observed both from space borne sensors and field work. These changes, primarily mass loss from the ice sheet, are related to the observed trend of earth's warmer climate in recent decades both in peer reviewed journals and in popular media.

This dissertation addresses two parameters that contribute to Greenland ice sheet mass balance estimates. The first factor is characterization of surface melting of the Greenland ice sheet from satellite-based passive and active microwave sensors. We use a wavelet based edge detection technique to delineate surface melt from brightness temperature measured by passive microwave sensors. Along with brightness temperature data, we also use normalized backscatter data from the Quick Scatterometer (QuikSCAT) as an independent sensor for comparison with the radiometer derived results. We use a semiempirical threshold based method for surface melt detection from QuikSCAT. Our results show a step-like, consistent increase in melt area of the Greenland ice sheet since 1995. This step-like increase is also observed in the mean summer air temperature along portions of the Greenland coast. The 1995 step-like increase of melt area (and melt index, a measure of melt intensity) is correlated with a distinct change of the North Atlantic Oscillation (NAO) index (from positive to negative) after 1995.

The second factor is mass accumulation in the upper reaches of the ice-sheet. We use an empirical model that correlates mean annual brightness temperature to annual accumulation rate. We apply a microwave emission model for the dry snow region of Greenland to show that 37 GHz vertically polarized brightness temperature data are better suited to capture the inter-annual variability of snow accumulation. Using our model we estimate a snow accumulation time series from brightness temperature for 150 km x 150 km area around Summit Camp in central Greenland. Using measured surface velocities and ice thickness we calculate the surface mass balance for our study area. We find a positive mass balance of 3.18 ± 6.0 cm/yr. Our mass balance derived elevation change is in agreement with satellite altimeter data and published results of other researchers.

因應全球暖化的課題，本篇闡述從空載微波感測器分析格陵蘭冰原地表積雪融化及雪的累積狀況。裡面提到主動式與被動式的微波感測器探測下進行的分類，以及堆積在冰原上游的累積品質。

Chapter3.Decadal Variations in NDVI and Food Production in India

Abstract

In this study we use long-term satellite, climate, and crop observations to document the spatial distribution of the recent stagnation in food grain production affecting the water-limited tropics (WLT), a region where 1.5 billion people live and depend on local agriculture that is constrained by chronic water shortages. Overall, our analysis shows that the recent stagnation in food production is corroborated by satellite data. The growth rate in annually integrated vegetation greenness, a measure of crop growth, has declined significantly ($p < 0.10$) in 23% of the WLT cropland area during the last decade, while statistically significant increases in the growth rates account for less than 2%. In most countries, the decade-long declines appear to be primarily due to unsustainable crop management practices rather than climate alone. One quarter of the statistically significant declines are observed in India, which with the world's largest population of food-insecure people and largest WLT croplands, is a leading example of the observed declines. Here we show geographically matching patterns of enhanced crop production and irrigation expansion with groundwater that have leveled off in the past decade. We estimate that, in the absence of irrigation, the enhancement in dry-season food grain production in India, during 1982–2002, would have required an increase in annual rainfall of at least 30% over almost half of the cropland area. This suggests that the past expansion of use of irrigation has not been sustainable. We expect that improved surface and groundwater management practices will be required to reverse the recent food grain production declines.

本篇NDVI的基本概念老師在上課的時候有教過，所以在讀這篇文章的時候比較容以理解。本篇闡述透過NDVI值觀測印度在1982年至2002年間的糧食產量的變化。

本研究表示，透過長期使用衛星、氣象及農作物觀測記錄影響糧食、水資源有限的熱帶地區最近停滯生產的空間分佈。分析表明，在糧食生產停滯是最近通過衛星資料證實。在每年的綜合增長率綠色植被，是作物生長的措施，在過去十年中顯著下降（P<0.10）在23%水資源有限的熱帶地區的耕地面積，而在經濟增長率顯著增加了不到2%以上。

Chapter4.Identification of Phytoplankton Pigment Assemblages Using Derivative Spectroscopy of Hyperspectral Remote -Sensing Reflectance

Abstract

One of the major challenges of ocean color research is distinguishing phytoplankton groups from in situ, airborne and satellite measurements to better understand diversity of phytoplankton and some involved biochemical processes. In this framework, high spectral resolution measurements of the remote-sensing reflectance, hyperspectral Rrs(λ), can potentially yield more information about the presence of diverse phytoplankton groups than can be gleaned from traditional analyses of single band-ratios at discrete wavelengths (i.e. multispectral approaches).

We introduce and discuss the feasibility of performing derivative spectroscopy and cluster analysis of hyperspectral Rrs(λ) to improve the automatic identification of phytoplankton populations in open ocean waters.

這篇文獻非常有趣，其敘述到利用高光譜遙感反射率導數光譜去判別浮游植物色素的聚集的識別方法。這裡面牽涉到老師教過我們的光譜的波段的圖的判別。研究者利用衛星影像判識浮游植物的葉綠素 a 的反應得到結果，以下是研究結果的成果圖：

Dominant accessory pigments to Chlorophyll *a*		Station Label
Fucoxanthin, 19'-Hex-Fucoxanthin		A
Divinyl Chl a, Zeaxanthin	(DV Chl a > Zea)	B
Divinyl Chl a, Zeaxanthin	(DV Chl a ≈ Zea)	C1,C2,C3,C4
19'-Hex-Fucoxanthin, Zeaxanthin	(19'-Hex-Fuco > Zea)	D
19'-Hex-Fucoxanthin, Zeaxanthin	(19'-Hex-Fuco ≈ Zea)	E
19'-Hex-Fucoxanthin, Fucoxanthin	(19'-Hex-Fuco > Fuco)	F

Table 1. Classification of stations into different groups based on phytoplankton community composition, as indicated by the ratios of two dominant accessory pigments to chlorophyll a.

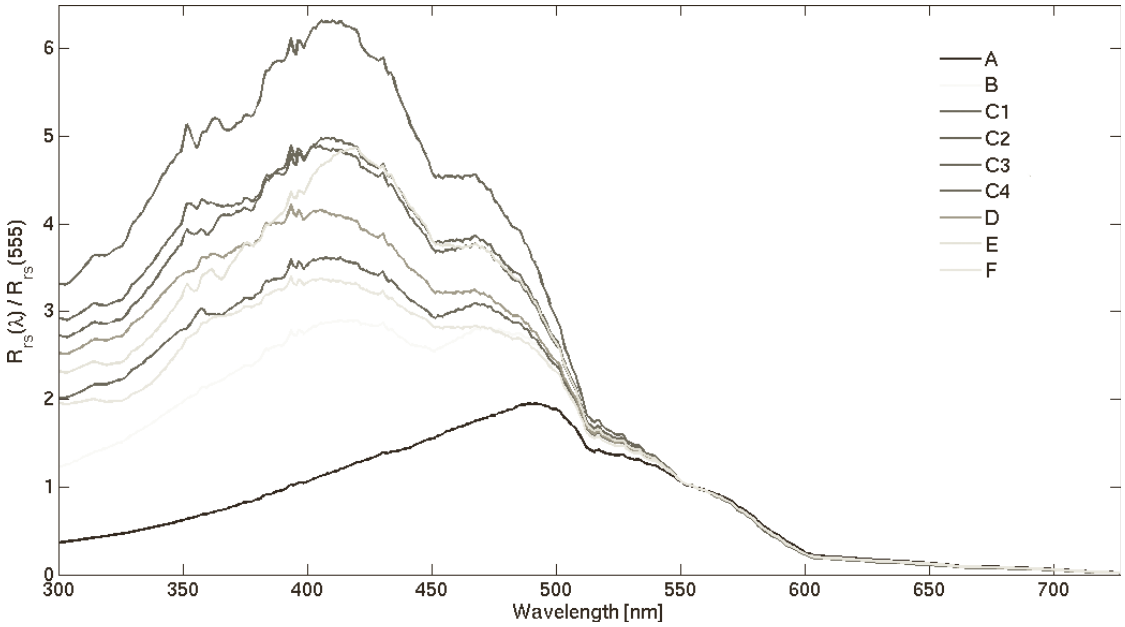

Figure 1. (a) Remote-sensing reflectance (Rrs(λ)) ratios computed for each group of stations (cf. Table 1).

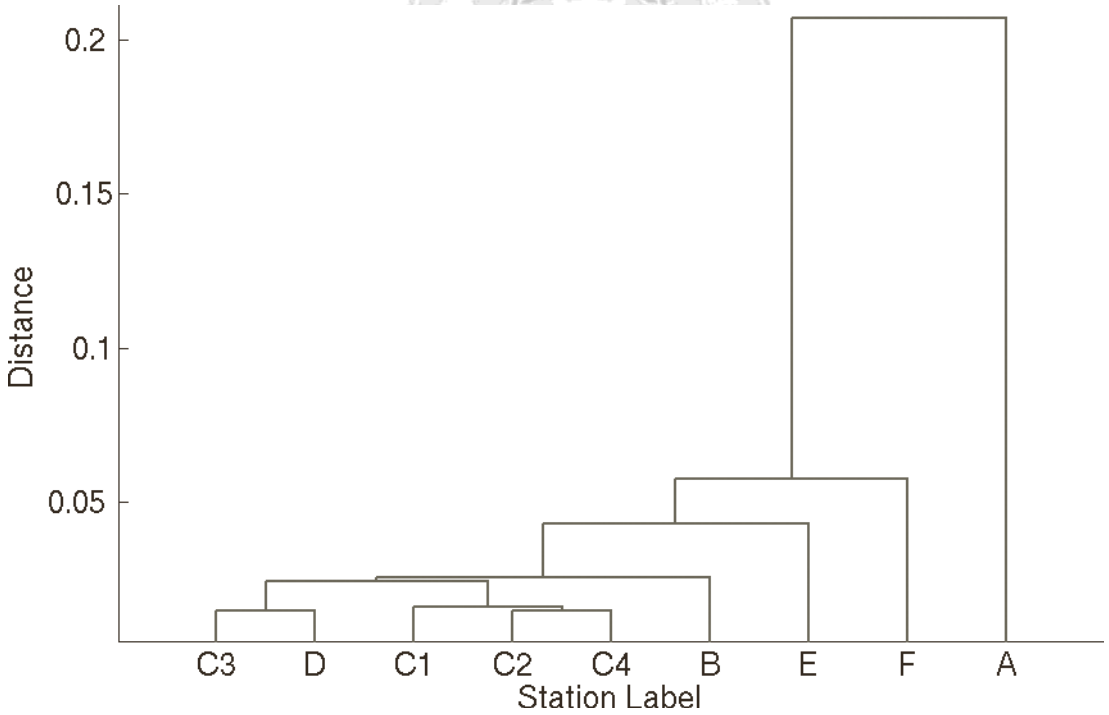

Figure 1. (b) Classification of stations based on hierarchical cluster analysis for second derivative of normalized hyperspectral Rrs(λ) spectra shown in Fig. 1(a).

Chapter5.以類神經網路建構定量降雨及多階段洪水預報模式

Abstract

The study built the real-time quantitative precipitation estimation/forecasting (QPE/F) from the meteorological radar data using recurrent neural network (RNN) and constructed the multi-step-ahead flood forecasting by training the back-propagation neural network (BPNN) utilizing the QPF information. First, a three-dimensional radar data structure which take into account the terminal velocity and the horizontal advection are used for training the RNN in QPE/F. The results of real-time rainfall estimation show that the RNN can produce much more accurate and stable performance than the Z-R power-law function. This work shows that the dynamic RNN can be applied successfully in real-time QPE/F using remote sensing data. Second, an exhilarating performance was found through the comparison of two recursive BPNN structures with different input patterns. This study demonstrates that the recursive structure with QPF outputs not only has the ability to improve the model accuracy but has the capability of reducing the time-delay problem that occurred in flood forecasting. Therefore, it is suggested that the recursive structure with the output of QPF is an effective method for multi-step ahead flood forecasting.

這篇論文雖然是以中文命題，但是內容是以英文撰寫，本研究首先以氣象雷達之觀測資料與回饋式類神經網路建立定量降雨預報模式，進而以預報之雨量值配合倒傳遞類神經網路架構五堵集水區多階段之洪水預測模式。在定量降雨預報模式上，藉由雷達觀測之回波建立三維輸入模型以訓練回饋式類神經網路，其中輸入模型之網格大小考慮雨滴終端速度及水準風速之影響，而網路輸出則為現時刻之即時雨量推估及下1-2 小時之雨量預報值，模式預報之準確度優於傳統之 Z-R 關係式。其次藉由評比兩組串列式架構之倒傳遞類神經網路可發現，網路在加入雨量預報值為額外之輸入時，不僅能改善多階段洪水預測之精確度，且在減少延遲現象的效應上亦可做有效地提升，本研究驗證在洪水預測模式之輸入模型上加入定量降雨預報之輸出，確實能提供模式有用之訊息，且有效地提供更為精確及穩定的多階段洪水預測成果。

Chapter6.圖繪田間水稻含氮狀態之遙感探測技術研究

Abstract

Nitrogen (N) is the most important nutrient to increase and stabilize yield of paddy rice, and the spatial distribution of N status of rice plants within field is the primary information needed for precision management of N fertilizer. A better yield production and grain quality can be expected by applying suitable amounts of N fertilizer at right time to the right place site-specifically with N map. This research was first to investigate changes in plant N concentration and leaf total chlorophyll content upon applying different rates of N fertilizer during rice (*Oryza sativa* L. cv. Tainung 67) growth, and then to examine whether the alterations in leaf internal structure and morphology related to variation in N status. The relations of leaf total chlorophyll content, internal structure and morphological characteristics, and plant N concentration to the canopy reflectance behavior were further studied. As the results shown, applying N fertilizer from 0 to 180 kg N ha^{-1}, with 60 kg N ha^{-1} intervals, changed leaf total chlorophyll and plant N concentration measured in the panicle initiation/formation stage. Plant applied with higher N rates tended to have higher amounts of leaf total chlorophyll and absorbed more light in the visible region of incident solar radiation. The mean reflectance of BLUE (425-490 nm), GREEN (490-560 nm) and RED (640-740 nm) wavebands showed a negative relationship with leaf total chlorophyll, a decreased in reflectance with the increase of chlorophyll content. A diversity of anatomical and morphological characteristics of leaves was observed to be modulated by N concentration in rice plants grown in both first and second cropping seasons. Leaf thickness increased progressively with increasing plant N concentration, and rice plants grown in second crop had a tendency to have thicker leaf blades than those grown in the first crop with the same N concentration. The extent of leaf rolling was relieved by the increasing N status and a linear relationship between value of leaf rolling index (LRI) and aboveground N concentration was fitted. Changes in bulliform/mesophyll ratio to aboveground N concentration were a quadratic function, the ratio increased to a plateau and decreased thereafter. Leaf water content (LWC) also changed in a curvilinear trend in the measured range of aboveground N concentration, and leaves of plants grown in first crop had higher LWC than those plants grown in second crop under

the same N level. A loose distribution and packing pattern of starch granules was found in the
parenchyma cells of plants with higher N status relative to those of lower N ones. Application of varied rates of N fertilizer also affected canopy reflectance behavior of different wavebands. The mean reflectance of waveband at BLUE, GREEN and RED decreased while NIR (740-1100 nm) increased with the increasing aboveground N concentration and LRI. Secondly, as the spatial distribution of canopy N map within a field is the primary information needed for precision management of N fertilizer, this research developed a simple spectral index (SI) using the first derivative values of canopy reflectance spectra at 735 nm ($dR/d\lambda_{735}$) to assess N concentration of rice plants and validated the applicability of a simplified imaging system based on the derived spectral model from the N─$dR/d\lambda|_{735}$ relationship in mapping canopy N status within fields from two remote sensing platforms. Results showed that values of $dR/d\lambda_{735}$ were linearly related to plant N concentrations measured at the panicle initiation/formation stage of first crop in 2001. The N─$dR/d\lambda_{735}$ relationship ($R^2 = 0.679$, $P < 0.001$) was better fitted than the N─NDVI (normalized difference vegetation index) relationship ($R^2 = 0.471$, $P < 0.010$), and remained valid ($R^2 = 0.514$, $P < 0.001$) when more data from different cropping seasons in varied years and locations were pooled . The composite regression model provided fair results ($r = 0.554$, $P < 0.010$) in validation test with another datasets collected from different crops and locations. The ratio-based SIs SRVI (simple ratio vegetation index) ($R^2 = 0.519$, $P < 0.001$), R_{810}/R_{560} ($R^2 = 0.453$, $P < 0.001$), NDVI ($R^2 = 0.355$, $P < 0.001$), and $(R_{1100}-R_{660})/(R_{1100}+R_{660})$ ($R^2 = 0.111$, $P < 0.010$) were also correlated with plant N concentration to a varied extent. Based on the as aforementioned N─NDVI relationship, a simplified imaging system, including an Electrim EDC-1000L monochrome camera, a Canon PHF6 1.4 lens, a set of Andover bandpass filters (730 nm and 740 nm), and an Advantech PCA6751 single board computer, was finally assembled and mounted on a mobile lifter and a helicopter to take spectral images of rice canopies for mapping the N status within fields. Results indicated that the system unit was able to provide field maps of canopy N status with reasonable accuracy ($r = 0.465$ to 0.912, RMSE = 0.100 to 0.550) from both remote sensing platforms. It appears that spatial information of N status obtained from this research may have a potential used for variable-rate applications of N fertilizer during the panicle initiation/formation stage. The validation tests on a variety of stress identification indices derived from

ground spectroradiometer measurements can also be easily performed with the established simplified imaging system following the process such as this research.

這篇論文雖然是以中文命題，但是內容是以英文撰寫，而且我發現看英文的摘要比較容易理解，可能作者的英文表達的比較好吧。這篇論文的摘要很長，寫了三頁，但是在摘要裡面把研究的精髓寫得很清楚。

研究者表示：氮素是提高和穩定水稻生產最重要的營養元素之一，田間水稻植株含氮狀態的空間分佈則系精准施用氮肥最主要的圖繪資訊。經由田間稻株含氮狀態空間分佈圖繪，將不等量氮肥於特定時間施用於農田特定位置的精准做法，將可預期獲得較佳之產量與米質。本研究首先調查田間栽培水稻生育期間施用不等量氮肥造成稻株植體含氮濃度及葉片葉綠素總量之改變，接著檢視葉片內部構造及形態隨著含氮狀態變化形成之差異，再進一步探討葉片葉綠素總量、內部構造與形態特徵、以及植體含氮濃度對植被反射比行為之影響。

在可見光不同波段反射比與葉片葉綠素總量的關係上，藍光(425-490 nm)、綠光(490-560 nm)及紅光(640-740 nm)波段之平均反射比皆與葉綠素總量呈現直線負相關，即各波段反射比隨葉綠素總量上升而下降。

經由本研究方法圖繪之穗起始期-形成期稻株含氮狀態空間變異分佈具有使用於可變率氮肥施用之應用潛力。

Chapter7. Canopy spectral invariants for remote sensing and model applications

Abstract

The concept of canopy spectral invariants expresses the observation that simple algebraic combinations of leaf and canopy spectral transmittance and reflectance become wavelength independent and determine a small set of canopy structure specific variables. This set includes the canopy interceptance, the recollision and the escape probabilities. These variables specify an accurate relationship between the spectral response of a vegetation canopy to the incident solar radiation at the leaf and the canopy scale and allow for a simple and accurate parameterization for the partitioning of the incoming radiation into canopy transmission, reflection and absorption at any wavelength in the solar spectrum. This paper presents a solid theoretical basis for spectral invariant relationships reported in literature with an emphasis on their accuracies in describing the shortwave radiative properties of the three-dimensional vegetation canopies. The analysis of data on leaf and canopy spectral transmittance and reflectance collected during the international field campaign in Flakaliden, Sweden, June 25—July 4, 2002 supports the proposed theory. The results presented here are essential to both modeling and remote sensing communities because they allow the separation of the structural and radiometric components of the measured/modeled signal. The canopy spectral invariants offer a simple and accurate parameterization for the shortwave radiation block in many global models of climate, hydrology, biogeochemistry, and ecology. In remote sensing applications, the information content of hyperspectral data can be fully exploited if the wavelength-independent variables can be retrieved, for they can be more directly related to structural characteristics of the three-dimensional vegetation canopy.

這也是一篇被刊登在 ELSEVIER 期刊內。題目是冠層光譜不變之遙感和模型應用。

文章提到以冠層光譜不變數的概念表現觀察葉片和冠層光譜透射和反射波長簡單的代數組合成為一個獨立，並確定冠層結構的一小部分特定變數的觀察。

Chapter8. Evaluation of Remote Sensing Based Terrestrial Productivity From MODIS Using Regional Tower Eddy Flux Network Observations

Abstract

The Moderate Resolution Spectroradiometer (MODIS) sensor has provided near real-time estimates of gross primary production (GPP) since March 2000. We compare four years (2000 to 2003) of satellite-based calculations of GPP with tower eddy CO2 flux-based estimates across diverse land cover types and climate regimes. We examine the potential error contributions from meteorology, leaf area index (LAI)/fPAR, and land cover. The error between annual GPP computed from NASA's Data Assimilation Office's (DAO) and tower-based meteorology is 28%, indicating that NASA's DAOglobal meteorology plays an important role in the accuracy of the GPP algorithm. Approximately 62% of MOD15-based estimates of LAI were within the estimates based on field optical measurements, although remaining values overestimated site values. Land cover presented the fewest errors, with most errors within the forest classes, reducing potential error. Tower-based and MODIS estimates of annual GPP compare favorably for most biomes, although MODIS GPP overestimates tower-based calculations by 20%–30%. Seasonally, summer estimates of MODIS GPP are closest to tower data, and spring estimates are the worst, most likely the result of the relatively rapid onset of leaf-out. The results of this study indicate, however, that the current MODIS GPP algorithm shows reasonable spatial patterns and temporal variability across a diverse range of biomes and climate regimes. So, while continued efforts are needed to isolate particular problems in specific biomes, we are optimistic about the general quality of these data, and continuation of the MOD17 GPP product will likely provide a key component of global terrestrial ecosystem analysis, providing continuous weekly measurements of global vegetation production.

Chapter9. 結合遙測技術與地理資訊系統以建立集水區降雨資料之推估模式之研究(Ⅲ)

中文摘要

本研究应用遥测技术之图像处理方法，辅以地理信息系统的空间及属性数据之分析功能以掌握集水区内各个雨量站控制范围之空间特性，如坡度、坡向、高程、距水源远近、纬度等，并依水文分布模式之原则，再配合统计分析方法，建立东部集水区雨量数据推估模式，以供集水区永续经营遥测水文学之研究与发展之参考。本研究所建立之雨量数据推估式分为两类：

1. 回归年25 年及50 年之年雨量数据推估模式
2. 回归年25 年及50 年短降雨延时之降雨强度数据推估式。

作者2000年在缘由与目的中提到：“台湾在人口持续增加的压力下，平地资源愈趋不敷使用，”这段话我想到现在少子化的社会人口结构来看已经不附合了。以前所有的规划及研究都是在人口增加的概念下的产物，在未来的规划及研究思想应该以“减”的思维去思考。但是作者后面的研究，的确有其研究价值。

本研究经回归分析完成之雨量推估模式，分为年雨量数据推估式及降雨强度数据推估式两类，如下表。年雨量资料推估式有回归年25 年及50 年之年雨量推估式；降雨强度数据推估式有回归年25 年降雨强度5 分钟、10 分钟、30 分钟及60 分钟之推估式。

表三 雨量站控制範圍空間因子

流域	站名	平均坡度(%)	平均坡向(°)	離水源最近距離(m)	高程(m)	緯度(°)
大武溪	紹家	15.69	205.72	6768	520.00	22.3967
知本溪	天鳥	3.38	163.58	7262	350.00	22.6694
知本溪	知本（5）	12.36	188.76	4485	100.00	22.6992
卑南溪	向陽	2.5	201.36	42944	2400.00	23.2581
卑南溪	霧鹿	4.23	220.73	33767	890.00	23.1694
卑南溪	新武（3）	9.83	241.35	24155	420.00	23.1331
卑南溪	武陵	5.58	150.38	17372	280.00	22.9694
卑南溪	上里	10.86	214.35	14546	220.00	22.8808
卑南溪	鹿鳴橋	19.43	184.06	12904	180.00	22.9011
卑南溪	台東	80.73	192.88	2046	40.00	22.7722
秀姑巒溪-富眾溪	樟原（1）	8.34	197.67	2550	120.00	23.4069
秀姑巒溪-富眾溪	忠勇	11.37	182.56	2282	120.00	23.3275
秀姑巒溪	卓麓	13.37	207.82	16866	210.00	23.2978
秀姑巒溪	苗圃	7.02	212.39	20415	940.00	23.4214
秀姑巒溪	立山	15.60	217.97	17086	180.00	23.4278
豐濱溪	豐濱	25.58	222.86	1202	30.00	23.6042
花蓮溪	西林	15.46	197.02	14017	200.00	23.8153
花蓮溪	銅門	20.36	199.38	11868	165.00	23.9667
三棧溪-美崙溪	北埔	18.04	182.46	2305	20.00	24.0375
和平溪	大濁水	11.12	160.97	3221	48.00	24.3308

表四 東部地區降雨資料推估模式

模式	相關係數 R
$P25 = -200956\ .375 + 2378\ .656\sqrt{S} + 100\ .231\sqrt{AS} + 469\ .321\sqrt{Lat} - 3788\ .331\sqrt{D} + 30\ .520\ H - 23\ .752\ \ln H$	0.851
$P50 = -185662\ .305 + 1987\ .367\sqrt{S} + 97\ .368\sqrt{AS} + 400\ .228\sqrt{Lat} - 2853\ .180\sqrt{D} + 25\ .364\ H - 12\ .587\ \ln H$	0.832
$I_{60}^{25} = 517\ .231 + 219\ .853\ S - 97\ .351\frac{1}{AS} + 0.218\ Lat^2 + 0.672 \times 10^{-3} D - 1.254\sqrt{H} + 0.225\ \ln H$	0.803
$I_{30}^{25} = 128\ .763 + 20\ .475\ S - 1045\ .331\frac{1}{AS} + 1.288\ Lat^2 - 4.574 \times 10^{-4} D - 0.373\sqrt{H} + 0.437\ \ln H$	0.712
$I_{10}^{25} = 1372\ .073 + 168\ .232\ S - 5863\ .725\frac{1}{AS} - 37.295\ Lat^2 - 5.726 \times 10^{-4} D - 3.132\sqrt{H} + 0.173\ \ln H$	0.778
$I_{5}^{25} = -9671\ .271 + 750\ .902\ S + 7568\ .483\frac{1}{AS} - 32.552\ Lat^2 - 0.369 \times 10^{-2} D + 62\ .209\sqrt{H} - 207\ .360\ \ln H$	0.528
$I_{60}^{50} = 337\ .159 + 157\ .779\ S - 136\ .62\frac{1}{AS} + 0.673\ Lat^2 + 2.369 \times 10^{-3} D - 2.897\sqrt{H} + 0.679\ \ln H$	0.791
$I_{30}^{50} = 98\ .275 + 37.792\ S - 1373\ .542\frac{1}{AS} + 0.921\ Lat^2 - 8.319 \times 10^{-3} D - 0.268\sqrt{H} + 0.327\ \ln H$	0.760
$I_{10}^{50} = 3712\ .285 + 377\ .078\ S - 6214\ .218\frac{1}{AS} - 33.707\ Lat^2 - 7.351 \times 10^{-3} D - 9.003\sqrt{H} + 3.752\ \ln H$	0.745
$I_{5}^{50} = 6312\ .936 + 502\ .562\ S - 1284\ .690\frac{1}{AS} - 17.197\ Lat^2 - 0.249 \times 10^{-4} D + 117\ .856\sqrt{H} + 1.237\ \ln H$	0.506

本研究利用地理資訊系統及遙感探測方法，提供整合空間及屬性資料與影像分析的技術，充分發揮遙測技術與地理資訊系統的優點，突破傳統方法之限制與缺失，以掌握中、上游集水區內各個雨量站之坡度、坡向、距海遠近等因數，配合不在同回歸年之總雨量及短延時降雨強度資料，應用以統計方法建立可適切反應臺灣北部地方河川中、上游集水區之降雨資料推估模式。

本研究中，我看到研究者如何去設立變相因數，如何去計算那些關係式。本研究也從前人的研究中獲得許多的方法及觀念，是對此研究很有幫助的。

Chapter10. The Moderate Resolution Imaging Spectroradiometer (MODIS): Land Remote Sensing for Global Change Research

Abstract

The first Moderate Resolution Imaging Spectroradiometer (MODIS) instrument is planned for launch by NASA in 1998. This instrument will provide a new and improved capability for terrestrial satellite remote sensing aimed at meeting the needs of global change research. The MODIS standard products will provide new and improved tools for moderate resolution land surface monitoring. These higher order data products have been designed to remove the burden of certain common types of data processing from the user community and meet the more general needs of global-to-regional monitoring, modeling, and assessment. The near-daily coverage of moderate resolution data from MODIS, coupled with the planned increase in high-resolution sampling from Landsat 7, will provide a powerful combination of observations. The full potential of MODIS will be realized once a stable and well-calibrated time-series of multispectral data has been established. In this paper the proposed MODIS standard products for land applications are described along with the current plans for data quality assessment and product validation.

找了多篇的研究文獻，發現 MODIS 跟 RS 很有相關，於是，找了 MODIS 的資料，以下是 MODIS 衛星資料簡介：

MODIS (or Moderate Resolution Imaging Spectroradiometer)是美國太空總署之 Terra 與 Aqua 衛星(圖)之重要酬載設備。由於衛星遙測與電腦電子技術能力的提升，在促進資源有效整合之前提下，MODIS 遙測資料係朝向整合大氣、海洋與陸地遙測資料整合的方向發展(modis.gsfc.nasa.gov)。為達到此一目的，該感應器之波段多達 36 個波段(表)，且隨著波段特性對大氣與海洋反射與吸收特性之不同，其應用也不相同，例如波段 1~2 應用於雲層之鑑別;波段 3~7 之應用則為陸地及雲層特性之探討,波長約為 459 nm~2155 nm；波段 8 ~16 (波長 400~900nm) 之應用則為葉綠素濃度分佈特性，而波段 31~32 則主要應用於海洋表面水溫資料的監測。此外，波段解析度亦有 250、500 及 1000 公尺之別，相較於 NOAA-AVHRR 及 SeaWiFS 資料而言，資料量十分龐大，所以其接收系統也從 L band 提升為 X band，相對地資料處理過程也相對複雜。目前本中心遙測實驗室之 MODIS 資料來源為中央氣象局衛星中心。

【 圖 酬載 MODIS 感應器之 Aqua（左）及 Terra（右)衛星 】

Primary Use	Band	Bandwidth[1]	Spectral Radiance[2]	Required SNR[3]
Land/Cloud Boundaries	1	620-670	21.8	128
	2	841-876	24.7	201
Land/Cloud Properties	3	459-479	35.3	243
	4	545-565	29.0	228
	5	1230-1250	5.4	74
	6	1628-1652	7.3	275
	7	2105-2155	1.0	110
Ocean Color/ Phytoplankton/ Biogeochemistry	8	405-420	44.9	880
	9	438-448	41.9	838
	10	483-493	32.1	802
	11	526-536	27.9	754
	12	546-556	21.0	750
	13	662-672	9.5	910
	14	673-683	8.7	1087
	15	743-753	10.2	586
	16	862-877	6.2	516
Atmospheric Water Vapor	17	890-920	10.0	167
	18	931-941	3.6	57
	19	915-965	15.0	250

Primary Use	Band	Bandwidth[1]	Spectral Radiance[2]	Required NEΔT(K)[3]
Surface/Cloud Temperature	20	3.660-3.840	0.45	0.05
	21	3.929-3.989	2.38	2.00
	22	3.929-3.989	0.67	0.07
	23	4.020-4.080	0.79	0.07
Atmospheric Temperature	24	4.433-4.498	0.17	0.25
	25	4.482-4.549	0.59	0.25
Cirrus Clouds	26	1.360-1.390	6.00	150[4]
Water Vapor	27	6.535-6.895	1.16	0.25
	28	7.175-7.475	2.18	0.25
	29	8.400-8.700	9.58	0.05
Ozone	30	9.580-9.880	3.69	0.25
Surface/Cloud Temperature	31	10.780-11.280	9.55	0.05
	32	11.770-12.270	8.94	0.05
Cloud Top Altitude	33	13.185-13.485	4.52	0.25
	34	13.485-13.785	3.76	0.25
	35	13.785-14.085	3.11	0.25
	36	14.085-14.385	2.08	0.35

Chapter11. Remote Sensing of Cloud, Aerosol, and Water Vapor Properties from the Moderate Resolution Imaging Spectrometer (MODIS)

Abstract

The Moderate Resolution Imaging Spectrometer (MODIS) is an earth-viewing sensor being developed as a facility instrument for the Earth Observing System (EOS) to be launched in the late **1990's.** MODIS consists of two separate instruments that scan a swath width sufficient to provide nearly complete global coverage every **2** days from a polar-orbiting, sun-synchronous, platform at an altitude of **705 km.** MODIS-N (nadir) will provide images in **36** spectral bands between **0.415** and **14.235** pm with spatial resolutions of **250** m **(2** bands), **500** m **(5** bands), and **1000** m **(29** bands). These bands have been carefully selected to enable advanced studies of land, ocean, and atmospheric processes. In this paper we describe the status of MODIS-N and its companion instrument MODIS-T (tilt), a tiltable cross-track scanning spectrometer with **32** uniformly spaced channels between **0.410** and **0.875** pm. In addition, we review the various methods being developed for the remote sensing of atmospheric properties using MODIS, placing primary emphasis on the principal atmospheric applications of determining the optical, microphysical, and physical properties of clouds and aerosol particles from spectral reflection and thermal emission measurements. In addition to cloud and aerosol properties, MODIS-N will be used for determining the total perceptible water vapor and atmospheric stability. The physical principles behind the determination of each of these atmospheric products will be described herein, together with an example of their application to aircraft and/or satellite measurements. Extensions of these and related methods to MODIS observations pose an extraordinary challenge as well as a unique opportunity to enhance our understanding of the earth-atmosphere-ocean system.

本研究非常有趣，其闡述中解析度成像光譜儀中的遙感探測之雲、氣溶膠和水蒸氣的性質。

本研究回顧了各種方法正在為利用 MODIS 大氣性質,把關於確定雲和氣溶膠粒子和光譜反射熱輻射測量的光學，微物理，物理性能主要大氣遙感應用的主要發展重點。除了雲和氣溶膠的特性，利用 MODIS - N 將被用於確定總感覺到水汽和大氣穩定。這些背後的每一個產品的測定大氣的物理原理將被描述外，連同他們的申請，例如飛機和/或衛星測量。這些和相關的方法擴展到 MODIS 衛星觀測構成非同尋常的挑戰，以及一個獨特的機會來加強我們對地球大氣，海洋系統的認識。

參考文獻

- Indrajit Bhattacharya, 2010, Analysis of Surface Melting and Snow Accumulation over the Greenland Ice Sheet from Spaceborne Microwave Sensors, UMI Dissertation Publishing, United State.
- Cristina Milesi, Arindam Samanta , Hirofumi Hashimoto , K. Krishna Kumar , Sangram Ganguly , Prasad S. Thenkabail , Ashok N. Srivastava , Ramakrishna R. Nemani and Ranga B. Myneni, 2010, Decadal Variations in NDVI and Food Production in India, Molecular Diversity Preservation International, Basel, Switzerland.
- E. Torrecilla, J. Piera1, D. Stramski, R. Reynolds, E. Millán-Nuñez, 2009, Identification of Phytoplankton Pigment Assemblages Using Derivative Spectroscopy of Hyperspectral Remote -Sensing Reflectances.
- Dong Huang, Yuri Knyazikhin , Robert E. Dickinson , Miina Rautiainen , Pauline Stenberg ,Mathias Disney , Philip Lewis , Alessandro Cescatti, Yuhong Tian , Wout Verhoef ,John V. Martonchik , Ranga B. Myneni, 2006, Canopy spectral invariants for remote sensing and model applications, Remote Sensing of Environment 106 (2007) 106–122.
- Faith Ann Heinsch, Maosheng Zhao, Steven W. Running, John S. Kimball, Ramakrishna R. Nemani, Kenneth J. Davis, Paul V. Bolstad, Bruce . Cook, Ankur R. Desai, Daniel M. Ricciuto, Beverly E. Law, Walter . Oechel, Hyojung Kwon, Hongyan Luo, Steven . Wofsy, Allison L. Dunn, J. William Munger, Dennis D. Baldocchi, Liukang Xu, David Y. Hollinger, Andrew D. Richardson, Paul C. Stoy, Mario B. S. Siqueira, Russell K. Monson, Sean P. Burns, and Lawrence B. Flanagan, 2006, Evaluation of Remote Sensing Based Terrestrial Productivity From MODIS Using Regional Tower Eddy Flux Network Observations, IEEE Transactions on Geoscience and Remote Sensing, vol. 44, No.7.
- Christopher O. Justice, Eric Vermote, , John R. G. Townshend, Ruth Defries, David P. Roy, Dorothy K. Hall, Vincent V. Salomonson, Jeffrey L. Privette, George Riggs, Alan Strahler, Wolfgang Lucht, Ranga B. Myneni, Yuri Knyazikhin, Steve W. Running, Rama R. Nemani, Zhengming Wan, Alfredo R. Huete, Wim van Leeuwen, Robert E. Wolfe, Louis Giglio, Jan-Peter Muller, Philip Lewis, and Michael J. Barnsley, 1998, The Moderate Resolution Imaging Spectroradiometer (MODIS): Land Remote Sensing for Global Change Research, IEEE Transactions on Geoscience and Remote Sensing, vol. 35, No.4.
- Michael D. King, Yoram J. Kaufman, W. Paul Menzel, and Didier Tanrk, 1992, Remote Sensing of Cloud, Aerosol, and Water Vapor Properties from the Moderate Resolution Imaging Spectrometer (MODIS), IEEE Transactions on Geoscience and Remote Sensing, vol. 30, No.1.
- 江衍銘、張斐章, 2007, 以類神經網路建構定量降雨及多階段洪水預報模式,

臺灣水利 第 55 卷 第 2 期，台灣。

- 李裕娟, 2007, 圖繪田間水稻含氮狀態之遙感探測技術研究
- 陳文福, 2000, 結合遙測技術與地理資訊系統以建立集水區降雨資料之推估模式之研究(Ⅲ)，行政院國家科學委員會專題研究計畫成果報告